Chapter 5

Three Dimensional Surface Ribbon Method

When the dimension of the structure is electrically small, the signal paths can be made short by sub-division and the quasi-static approach is sensible for the calculation of equivalent circuit models. For the simple case of non-parallel lines, as mentioned earlier, the volume filament method (VFM) is applicable with rather complicated integration of Green's function as in [61]. Discontinuities such as a microstrip line bend, via-hole, etc. have been examined using the integral equation method assuming perfect conductors and using scalar current potential or scalar magnetostatic potential as state variables [68, 69]. For general structures frequency dependent resistance and inductance can be obtained by solving the volume current integral equation in three dimension, which is known as the partial element equivalent circuit method (PEEC) [54, 60, 64, 70-73]. Full-wave techniques have also been applied to analyzing three dimensional geometries, but at the expense of increased numerical burden. The full-wave spectral domain method (SDM) has been used in analyzing a spiral inductor having an air-bridge, with the assumption of perfect conductors [74]. The electric field integral equation (EFIE) using the standard impedance boundary condition (SIBC) has also been developed for characterizing three dimensional structures of microstrip line, via, and meshed reference plane at high frequency [9, 10, 54, 75]. The finite difference time domain method (FDTD) has been used to characterizing discontinuities and reference planes [76-79].

In the previous chapter, the effective internal impedance (EII) was successfully combined with the current integral equation and it significantly reduced computation

time. This approach can be extended into three dimensional geometries under the quasi-static assumption [80]. In this chapter, EII will be defined for all ribbons on the surfaces of the conductor according to the direction of current flows, the surface current integral equations will be derived, and the current continuity condition will be applied. This three dimensional surface ribbon method (3DSRM) can be utilized where PEEC can calculate frequency dependent resistance and inductance, such as the discontinuities of bend and simple via, various reference planes, meander lines, etc. The efficiency and accuracy of this 3DSRM will be examined through examples of right-angled bends, meander lines, and a microstrip line with a meshed ground plane. For comparison PEEC will be applied and the volume filament method (VFM) will be used with a two dimensional approximation.

5.1 Partial Element Equivalent Circuit Technique

Ruehli [70] developed the partial element equivalent circuit method (PEEC) for evaluating capacitance and frequency dependent resistance and inductance of three dimensional geometries. And recently he has proved that the full-wave form of PEEC is no more than exploiting the method of moments [81, 82]. He also derived a quasi-static form of PEEC and applied it to evaluating resistance and inductance of a microstrip line bend [71] and ground plane connections [60]. This approach is based on the volume current integral equation using current vector as state variables, shown in (4.6). Current continuity condition is enforced by applying Kirchhoff's current law or voltage law, and, therefore, a nodal-based or mesh-based matrix is formed to be solved. Also hybrid finite element method and method of moments was developed to solve this volume integral equation in two steps instead of nodal-based or mesh-based

approach, and has been utilized to solve a microstrip bend and simple shaped vias [83].

Recently, PEEC has been applied to calculating the frequency dependent inductance of a ceramic quad flat pack (CQFP) having about 200 pins, considering the skin effect of the non-straight signal paths and frequency dependent current distribution on a ground plane [84]. And it has been utilized to calculate the inductance of a via [85] and can also be applied to the effective inductance evaluation of reference planes presented in [86, 87] for the evaluation of simultaneous switching noise. But PEEC needs an increasing number of segments to appropriately account for frequency dependent resistance and inductance due to the skin and proximity effects at high frequency and for complicated structures. To reduce the numerical complexity thick conductors can be replaced by a thin strip and sheet resistance as in [84], which is applicable for limited structures and does not accurately capture the high frequency resistance.

Instead of approximating the structure a preconditioned generalized minimal residual (GMRES) algorithm or a conjugate gradient algorithm can be adopted as a fast iterative matrix solver, instead of expensive direct matrix solvers such as gaussian elimination or LU decomposition. The speed of this approach can be enhanced with the use of a multipole-accelerated algorithm for fast and approximated matrix-vector multiplication [64]. Also PEEC has been speeded up more by a FFT-based algorithm for matrix-vector multiplication in case of an uniformly segmented arbitrarily shaped reference plane [72, 73]. To capture the finite conductivity and the skin and proximity effects fine discretization is required and it could be avoided by extending the

SRM into three dimensional geometries. In addition, numerically efficient techniques can be incorporated with SRM as well as PEEC.

5.2 Three Dimensional Surface Ribbon Method

Instead of solving the volume current integral equation inside of the conductor in PEEC, only the surface of the conductor is segmented into ribbons and at each ribbon and along the current flow direction EII is defined to represent the characteristics of the conductor interior, as in two dimensional problem. Unlike the two dimensional problem where the current continuity condition is inherently satisfied, this condition should be enforced in the surface current integral equations as in PEEC. In following sub-sections, the segmentation scheme of 3DSRM will be explained compared to PEEC, the EII will be defined using the transmission line model, and mesh-based analysis will be considered.

5.2.1 Discretization and Effective Internal Impedance

In PEEC, the conductor is divided into small hexahedrons as shown in the right-angled bend structure of Fig. 5.1(a), a node is placed at the center of each hexahedron, and a partial element is defined between two adjoining nodes, as shown in Fig. 5.1(b). The volume current integral equation is expanded and tested at each element using pulse basis functions and, therefore, three dimensional current flow is considered in-side of the conductor. In 3DSRM, the conductor surface is divided into rectangular patches as in Fig. 5.2(a), a node is also given at the center of each rectangular patch, and a ribbon is defined between two adjoining nodes as in Fig. 5.2(b). Therefore, the number of segments is reduced by replacing volume discretization of the order N^3 in PEEC by surface discretization of the order N^2 in 3DSRM.

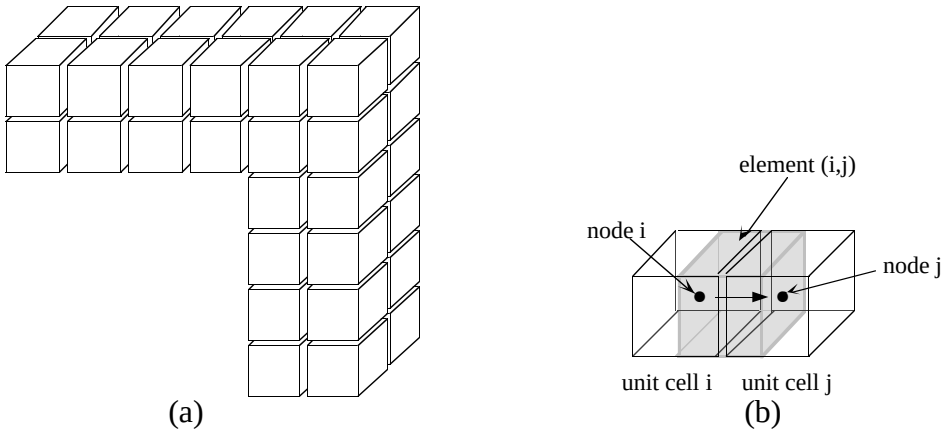

Figure 5.1: Discretization of the conductor inside for the use of partial element equivalent circuits (PEEC) method in an example of a right-angled bend. (a) The conductor is divided into small hexahedrons, and (b) an element is defined between adjoining nodes placed at the center of the hexahedrons; arrow indicates direction of current flow.

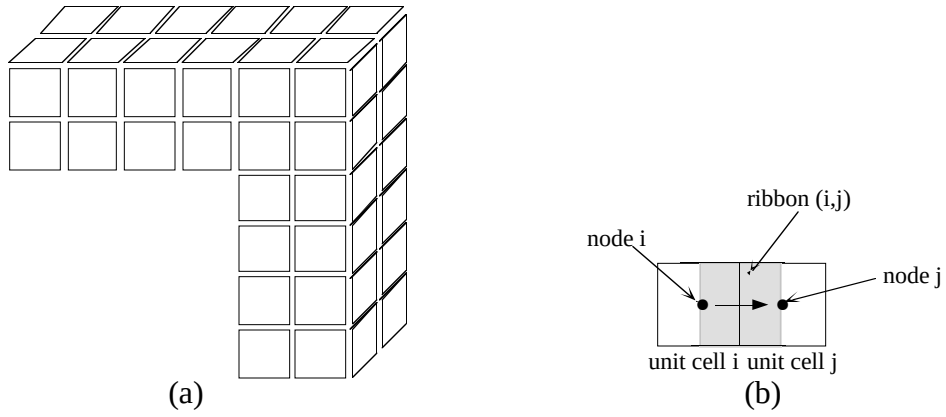

Figure 5.2: Discretization of the conductor surface for the use of the three-dimensional surface ribbon method (3DSRM) in an example of a right-angled bend. (a) The conductor surface is divided into small rectangular patches, and (b) a ribbon is defined between adjoining nodes placed at the center of the rectangles; arrow indicates direction of current flow.

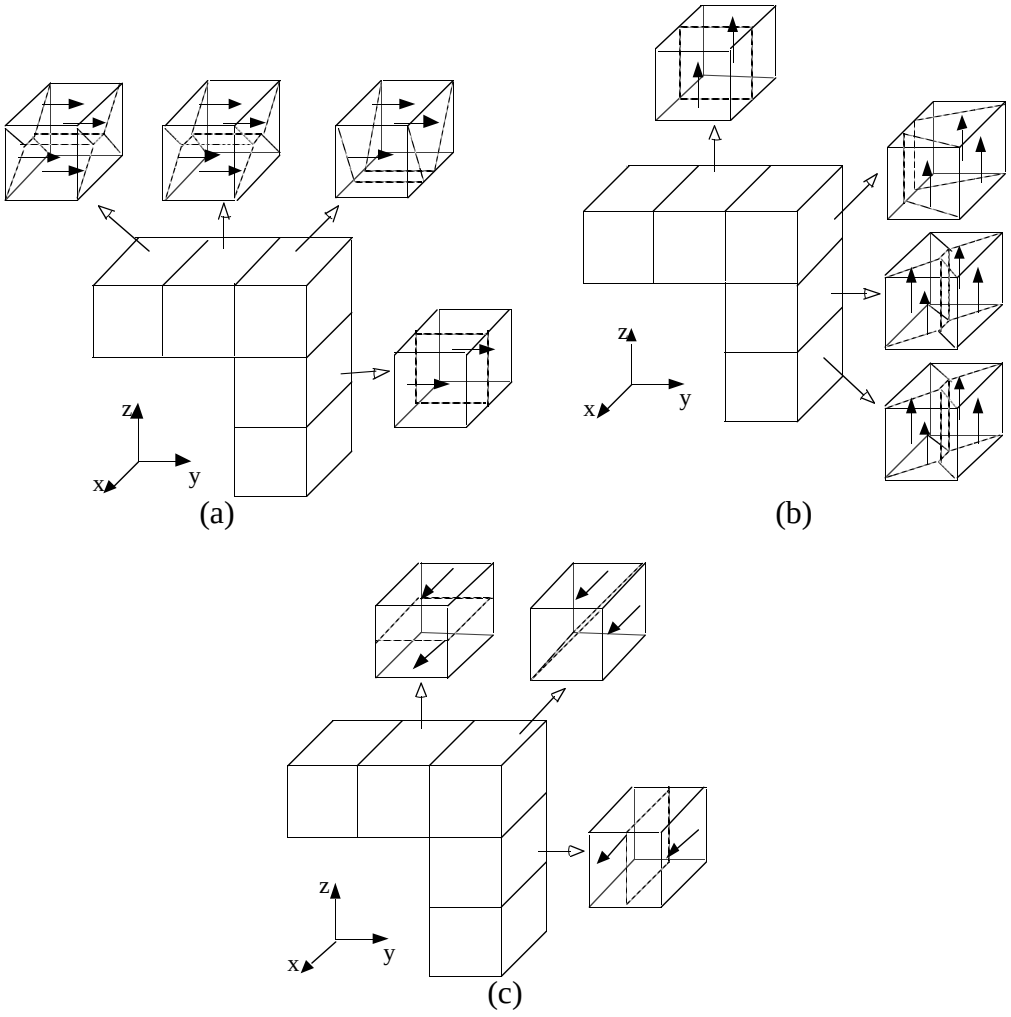

Figure 5.3: Sub-divisions of the conductor interior for defining the effective internal impedance (EII) along the direction of current flows in an example of a right-angled bend. (a) y-axis, (b) z-axis, (c) x-axis; arrows indicate direction of current flow.

Based on the above discretization scheme, two directional surface current is defined all over the surface of the conductor. And on each ribbon EII should be assigned the appropriate modeling corresponding to the direction of the surface current. One possible way to define EII on three dimensional geometries is to approximate the surface impedance of the structure, but it is hard to guess the surface impedance be-

cause of the complicated geometries. As in reference [20] and Chapter Two the plane wave model could be modified or extended to account for arbitrary three dimensional geometries. Or the transmission line model in Chapter Two could be extended into three dimensional geometries. In this study, the transmission line model is easily extended into three dimensional structures. Figure 5.3 shows how to divide the conductor interior for EII models along all directions of the current for an example of a right-angled bend. At and near the corner two tangential currents are defined and for uniform sections only longitudinal current is assumed. Where the number of outer surfaces are four, EII is defined as in two dimensional problems. If the number of outer surfaces are three, then the rectangular cross-section is divided into two pairs of isosceles triangles near two corners of adjoining surfaces and flat rectangles for what remains. For adjoining two surfaces it is divided into two isosceles triangles at the corner and two flat rectangles for what remains, and for two parallel surfaces it is divided into two flat rectangles. For each isosceles triangle EII is derived using the transmission line model, and for each rectangle the surface impedance of a flat conductor is used as explained in Chapter Two.

5.2.2 Current Continuity Condition and Mesh Analysis

The surface current integral equation of (4.12) is driven at each ribbon. The impedance matrix can be deduced by relating current and voltage at each ribbon as follows

$$[Z][I_r] = [V_r], \tag{5.1}$$

where $[V_r]$ and $[I_r]$ are $n \times 1$ ribbon voltage and current vectors, n is the number of ribbons, and $n \times n$ impedance matrix of $[Z]$ is given by

$$[Z] = [Z_{eii}(\omega)] + j\omega[L] \tag{5.2}$$

To ensure the current continuity condition, Kirchhoff's voltage law (KVL) is applied to the matrix equation of (5.1) that then leads to mesh analysis, which has fewer unknowns and a more regular matrix than the nodal analysis using Kirchhoff's current law (KCL). KVL is expressed using the mesh matrix relating each ribbon and meshes by

$$[M][V_r] = [V_m] \tag{5.3}$$

where $[M]$ is the $m \times n$ mesh matrix, $[V_m]$ is the $m \times 1$ mesh voltage vector, and m is the number of meshes. The mesh voltages are almost zero except the meshes where external sources are applied. Also current on each ribbon is related to mesh currents using the above mesh matrix as follows

$$[M]^t[I_m] = [I_r], \tag{5.4}$$

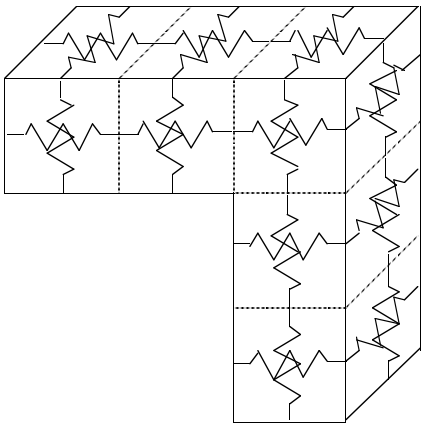

Figure 5.4: Circuital representation of the three-dimensional surface ribbon method (3DSRM) in case of a right-angled bend.

where $[I_m]$ is the $m \times 1$ mesh current vector. Finally, the mesh matrix equation is formed by

$$[M][Z][M]^t[I_m] = [V_m] \tag{5.5}$$

The above procedure is identical to the mesh analysis [64] in PEEC, and frequency dependent resistance and inductance are obtained by solving the above matrix with direct or iterative matrix solvers. Figure 5.4 shows the equivalent circuits of the mesh analysis for an example of a right-angled bend.

5.3 Examples

The accuracy and efficiency of 3DSRM could be shown by characterizing discontinuities and complex planar structures of high frequency circuits. Because the quasi-static approximation is valid not only for uniform lines but also for discontinuities such as bends and vias, a lumped circuit model can be used to represent the discontinuities. First, coupled right-angled bends are examined as one of the simplest cases. When the planar structure becomes complicated and the non-uniform parts are not negligible, the non-uniform structures can not be simplified into uniform lines. The series impedance of coupled meander lines are analyzed as a complicated case. And a microstrip line with a meshed ground plane is examined to see the effects of mesh pitch and apertures. For comparisons PEEC is used and the volume filament method (VFM) is also applied, but this requires simplifying the geometries.

5.3.1 Coupled Right-angled Bends

Figure 5.5 shows coupled right-angled bends, where the rectangular conductors are 10 μm wide and 10 μm thick, placed on a plane with gap of 10 μm, and conduc-

tivity 5.8×10^7 [S/m]. For that structure resistance and inductance are calculated by 3DSRM, PEEC, and approximated using VFM, To distinguish bend discontinuities from uniform lines two reference planes are placed from the corner of outer lines at a distance l_d = 35 μm. These planes are selected where the current distribution is within 10% that of uniform lines VFM simplifies the structure into two pairs of straight lines with length chosen to give correct DC resistance. The "excess" resistance and inductance of the bends are obtained by subtracting the impedance of uniform lines from the total impedance as follows

$$\begin{aligned} R_{dis} &= R_{tot} - R_{uni} \\ L_{dis} &= L_{tot} - L_{uni} \end{aligned} \tag{5.6}$$

where R_{tot} and L_{tot} are the total resistance and inductance, and R_{uni} and L_{uni} are the resistance and inductance of two pairs of twin uniform lines with the length of $l - l_d$. Resistance and inductance of uniform lines are calculated with VFM for PEEC and

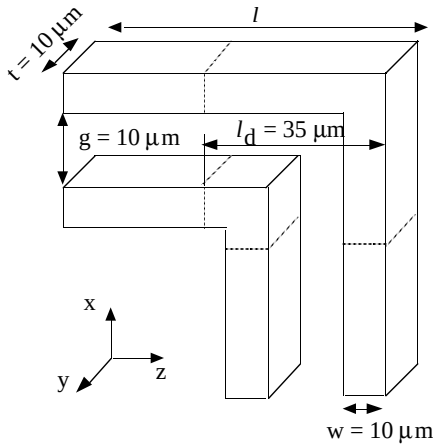

Figure 5.5: Coupled right-angled bends. The lines are 10 μm wide, 10 μm thick, 10 μm spacing, and conductivity 5.8×10^7 [S/m]. Discontinuity section is defined on the bends from the corner of outer lines with l_d = 35 μm.

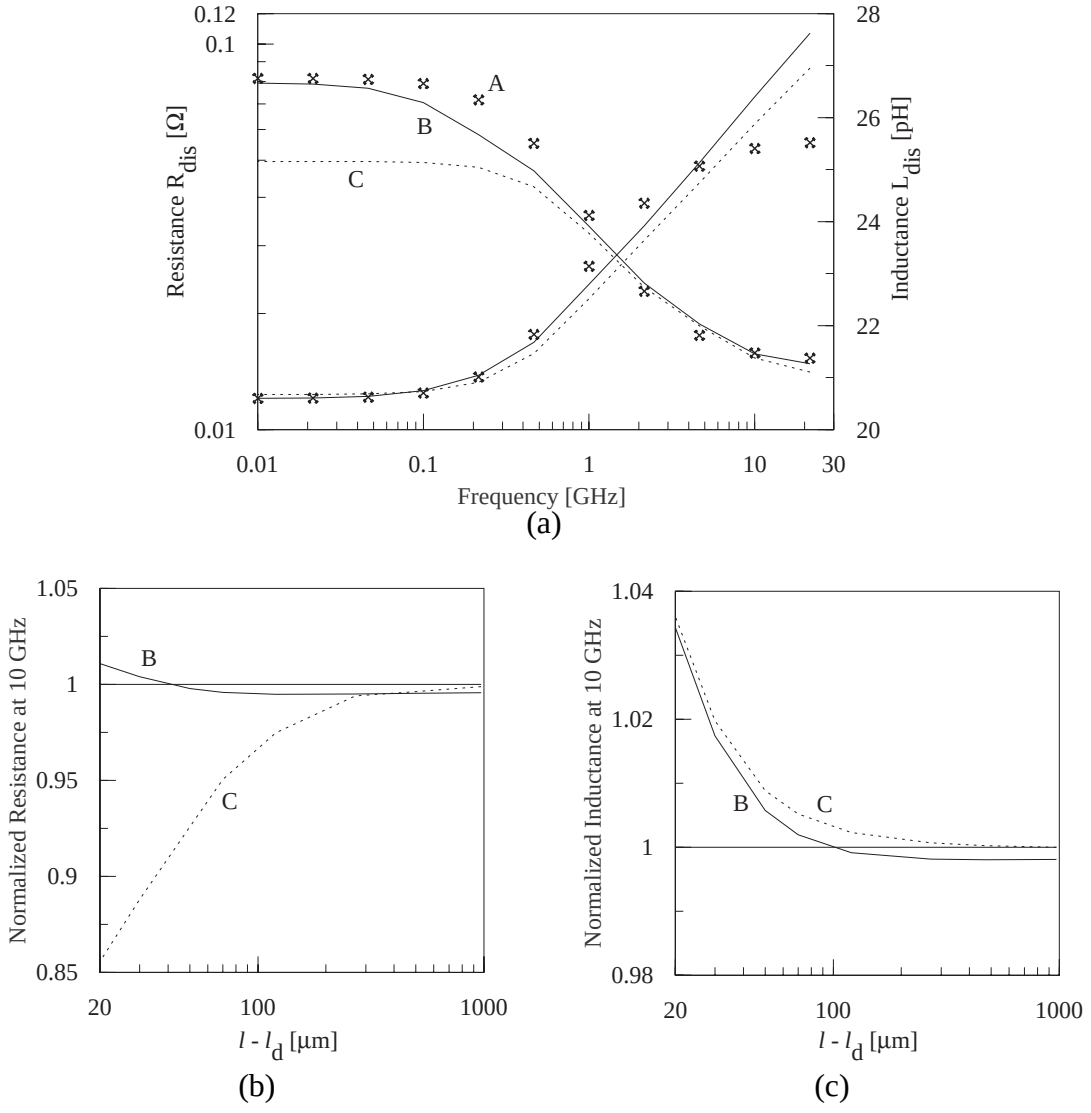

Figure 5.6: Comparison of resistance and inductance of coupled right-angled bends between partial element equivalent circuits method (PEEC), three-dimensional surface ribbon method (3DSRM), and two-dimensional approximation using the volume filament method (VFM). (a) Discontinuity resistance and inductance with $l - l_d$ = 100 μm, (b) Total resistance normalized by resistance, (c) Total inductance normalized by inductance of uniform lines having the same DC resistance. A(⋇): PEEC; B(solid line): 3DSRM; C(dotted line): 2-D approximation using VFM.

VFM, and two dimensional SRM for 3DSRM with the same segmentation scheme. PEEC uses uniform 4×4 segments at each side of the conductor and 9 segments longitudinally, VFM uses uniform 10×10 segments, and 3DSRM uses uniform 3 segments at each surface of the conductor. This leads 973, 249, and 199 unknowns for PEEC, 3DSRM, and VFM, respectively. Figure 5.6(a) shows resistance and inductance and compares with each technique used, when the length $l - l_d$ is 100 μm. For discontinuity inductance 3DSRM is close to PEEC with a deviation of less than 2%, and VFM is off 6% at low frequency and agrees well at high frequencies. For discontinuity resistance PEEC does not capture the skin effect fully at high frequency due to coarse segments, and VFM give quite close answer to 3DSRM with 20% error.

For this simple bend having small non-uniform parts compared to uniform parts, the discontinuities do not have significant effect under the quasi-static assumption. To see the effect of bends, total resistance and inductance are normalized, respectively, by resistance and inductance of twin uniform lines having the same DC resistance as that of the original lines. Impedance of twin uniform lines is calculated by SRM with 7 segments on each side of the conductor. Figure 5.6(b) compares normalized resistance and Fig. 5.6(c) shows normalized inductance at the high frequency of 10 GHz. As shown in the figures, discontinuity resistance and inductance can be simply approximated by straight lines having the same DC resistance for a line length longer than 100 μm.

5.3.2. Coupled Meander Lines

Like the rectangular spiral inductor in reference [74], the corners of meander lines with short uniform sections may have significant effect on frequency dependent resistance and inductance. When the meandering is periodically repeated, one period

is named the unit cell; two periods of coupled meander lines are drawn in Fig. 5.7. The rectangular conductor is 10 μm wide and 10 μm thick, the pitch of a period is 40 μm, two lines are spaced with gap of 10 μm, and the conductivity is 5.8×10^7 [S/m]. Because of the periodicity of the structure the periodic condition can be enforced into the current integral equations, and again the number of unknowns can be reduced by a half due to mirror image symmetries. Thus, the number of unknowns can be kept to that of unit cell regardless of the line length. The surfaces of lines is expressed by unit cell geometries as follows

$$S_{all}(x,y,z)=\sum_{i=0}^{1}\sum_{k=0}^{nc}S_{uc}\left((-1)^i x,y,z+kP\right), \tag{5.7}$$

where S_{all} is the surface of the entire lines, S_{uc} is the surface of a unit cell, nc is the number of periods, and P is the pitch of a period. Therefore, the matrix equation of (4.13) can be rewritten as follows

$$\left(\left[Z_{eii}\left(r(x,y,z)\right)\right]+j\omega\sum_{i=0}^{1}\sum_{k=0}^{nc}\left[L\left(r(x,y,z),r'\left((-1)^i x',y',z'+kP\right)\right)\right]\right)\left[I_r\right]=\left[V_r\right] \tag{5.8}$$

where $r(x,y,z),r'(x',y',z')\in S_{uc}$. The above periodic condition requires more time for assembling the matrix as the line length increases, but the number of unknowns remains the same and matrix solving time is constant.

Resistance and inductance of meander lines with 10 cells has been calculated using 3DSRM, PEEC, and approximated using VFM. Figure 5.8(a) shows resistance and inductance per period and compares the results with each other. Like in the case of right-angled bends VFM uses the simplified structure of cascaded straight lines giving correct DC resistance. PEEC uses uniform 5×4 segments at each side of the

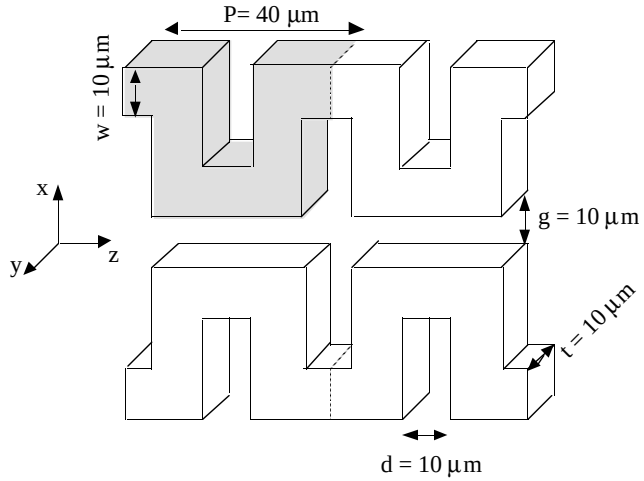

Figure 5.7: Coupled meander lines. The lines are 10 μm wide, 10 μm thick, 10 μm spacing, 40 μm period, and conductivity 5.8×10^7 [S/m]. Two lines are mirror symmetric against yz-plane with x=0.

conductor, VFM uses uniform 10×10 segments, and 3DSRM uses uniform 3 segments at each surface of the conductor. This leads to 1021, 209, and 397 unknowns for PEEC, 3DSRM, and VFM, respectively. For inductance 3DSRM is close to PEEC with deviation of less than 3%, and VFM is considerably off 26% due to underestimated line length. For resistance 3DSRM and PEEC are matched well up to about 3 GHz, within 3%, and beyond that PEEC does not capture the skin effect fully due to coarse segments, and VFM is off 30% from 3DSRM. Figure 5.8(b) compares inductance vs. line length. When the line length becomes longer than 5 times the period, per unit period inductance reaches a constant value. And 3DSRM and PEEC give almost same low frequency inductance, are about 3% different for the high frequency inductance, and VFM underestimates inductance about 26%. In Table 5.1 the number of unknowns and the computation time are compared. It shows 3DSRM significantly reduces the number of unknowns and CPU time over PEEC and even VFM of two dimensional approximation.

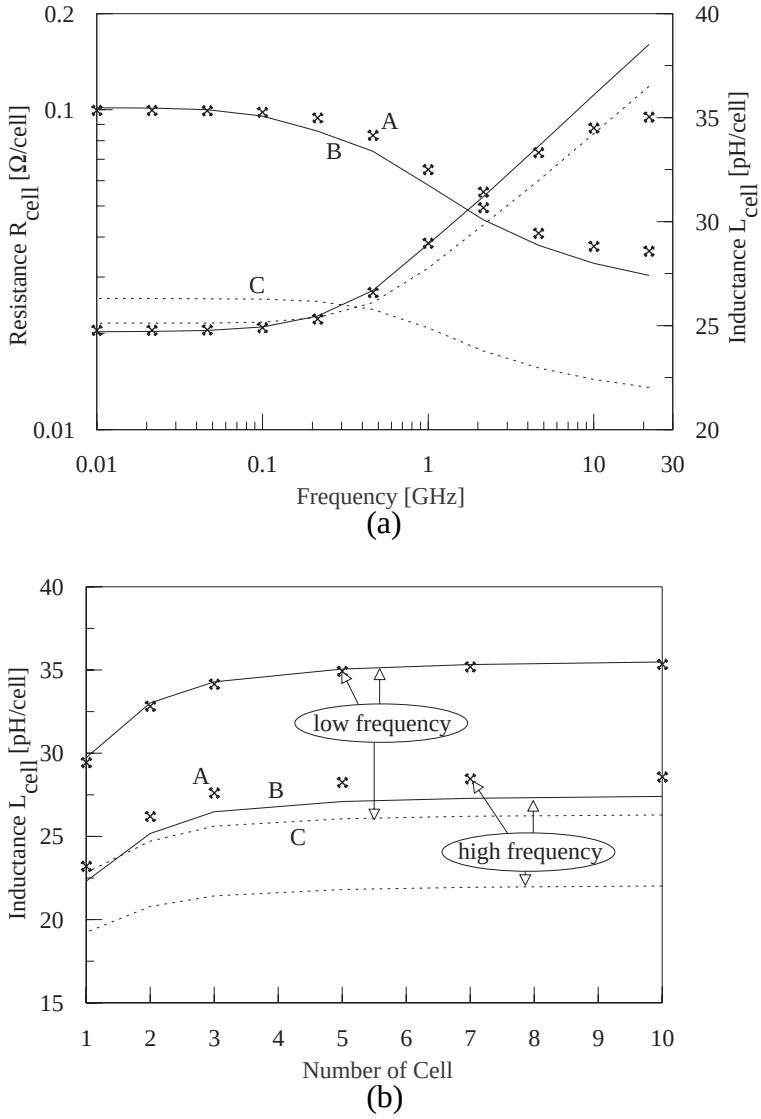

Figure 5.8: Comparison of resistance and inductance of coupled meander lines between partial element equivalent circuits method (PEEC), three-dimensional surface ribbon method (3DSRM), and two-dimensional approximation using the volume filament method (VFM). (a) Per unit period resistance and inductance calculated with 10 periods, (b) Per unit period inductance calculated vs. the number of periods. A(⋇): PEEC; B(solid line): 3DSRM; C(dotted line): 2-D approximation using VFM.

Method	Number of unknowns	CPU time[sec] Assembling*	Solving per freqeun
PEEC	1021	5234	415
3D SRM	209	57	7.5
2D VFM	397	667	26

Table 5.1: Comparison of the number of unknowns used and run times on an IBM RISC 6000 for partial element equivalent circuits method (PEEC), three-dimensional surface ribbon method (3DSRM), and 2-D approximation using the volume filament method (VFM). Gaussian elimination is used as a matrix solver, and * is in case of 5 periods.

5.3.3 A Microstrip Line over a Meshed Ground Plane

The electromagnetic modeling of a transmission line structure with a reference plane have been widely studied through quasi-TEM or full-wave techniques in the two-dimensional domain. The meshed plane instead of the solid plane has become an important structure in modern microelectronic packaging such as deposited metal-organic multichip modules (MCM-Ds), which is to obtain desired electrical and mechanical characteristics with less metal coverage and thinner dielectric layer. However, the transmission line over a meshed reference plane is more difficult to analyze than the transmission line over a solid plane due to the complicated mesh pattern. Full-wave electrical field integral equation (EFIE) methods [10, 75, 88] and the finite difference time domain (FDTD) method [77] have been utilized to analyze a periodically perforated reference plane, and some measurements have been performed [89]. And a simple analytic approach [90] has also been applied to evaluate the propagation constant where the transmission line over a meshed ground plane is approximated by cascading two uniform transmission lines which are easily analyzed by two-dimen-

sional quasi-TEM field solvers. But the studies are mainly focused on calculating high frequency characteristic impedance and propagation constant, frequency dependent loss, so the effect of the reference plane have not been fully examined. In this section, 3DSRM as well as PEEC is applied to calculate frequency dependent resistance and inductance of the transmission line over a periodically perforated ground plane.

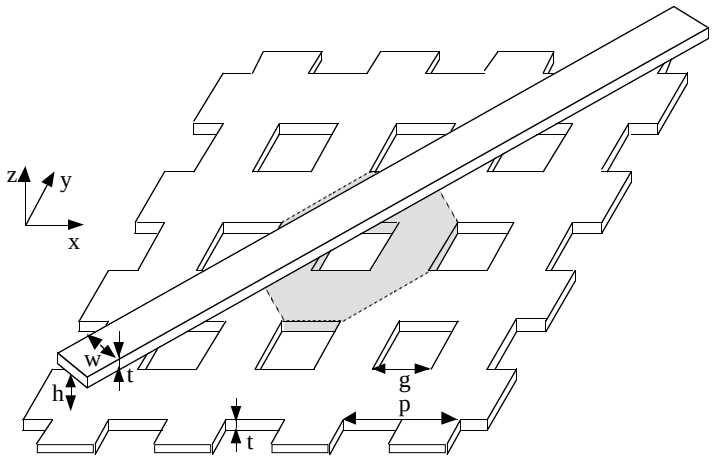

Figure 5.9: A microstrip line over a meshed ground plane where the aperture is placed at an angle of 45° with respect to the signal line. The signal line is 12 μm wide, 2.5 μm thick, 12 μm over the ground, the mesh pitch is 100 μm, the aperture is 50 μm square, and the conductivity is 5.8×10^7 [S/m].

Figure 5.9 shows part of a microstrip line over an obliquely oriented meshed ground plane, where the signal line is 12 μm wide, 2.5 μm thick and 12 μm over the ground plane, the ground plane has the mesh pitch of 100 μm, an aperture of 50 μm square, the signal line is 45° with respect to x-axis, and the conductivity is 5.8×10^7 [S/m]. The shaded part is a unit ground cell with the period of $100\sqrt{2}$ μm, so the periodic condition is utilized as in 5.3.2. Resistance and inductance of this structure with 5 apertures perpendicular to the signal line and 9 apertures along the signal line

were calculated by PEEC and 3DSRM. Figure 5.10 shows resistance and inductance per unit length and compares the results with each other and a microstrip line over a solid ground. PEEC exploits three different segmentation schemes. First, the meshed ground is approximated by connecting straight lines and 6×3 segments are used at each side of the conductor with width ratios of 3 and 2.5, respectively. Second, one unit cell of the meshed ground is segmented by uniform 9×9 segments on xy-plane and one layer segment is used along the z-axis. Third, one unit cell of meshed ground is segmented by uniform 9×9 segments on xy-plane and two layer segments are used along the z-axis. The signal line is non-uniformly segmented into 12×4

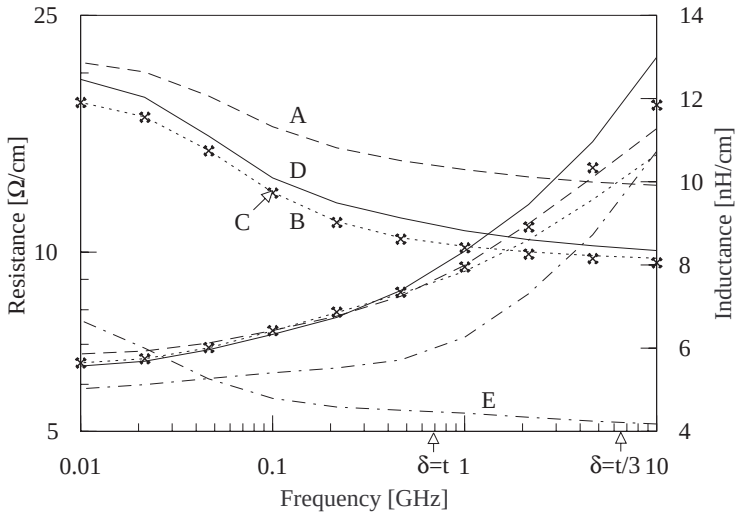

Figure 5.10: Comparison of resistance and inductance of a microstrip line over a meshed ground plane between partial element equivalent circuits method (PEEC), three-dimensional surface ribbon method (3DSRM), and a microstrip line over a solid ground. A(dashed line): PEEC with straight line approximation; B(dotted line): PEEC with one layer segment of the ground; C(⋇): PEEC with two layer segments of the ground; D(solid line): 3DSRM, E(dot-and-dashed line): a microstrip line over a solid ground. Meshed ground is considered by 5 apertures perpendicular to the signal line and 9 apertures along the signal line.

Method	Number of unknowns	CPU time[sec] Assembling*	Solving per freqeun
PEEC1	398	1360.1	18.6
PEEC2	283	1788.4	8.0
PEEC3	743	4745.1	146.7
3D SRM	148	37.2	3.1

Table 5.2: Comparison of the number of unknowns used and run times on an IBM RISC 6000 for three segmentation schemes of partial element equivalent circuits method (PEEC) and three-dimensional surface ribbon method (3DSRM). Gaussian elimination algorithm is used as a matrix solver, and * is in case of 9 periods.

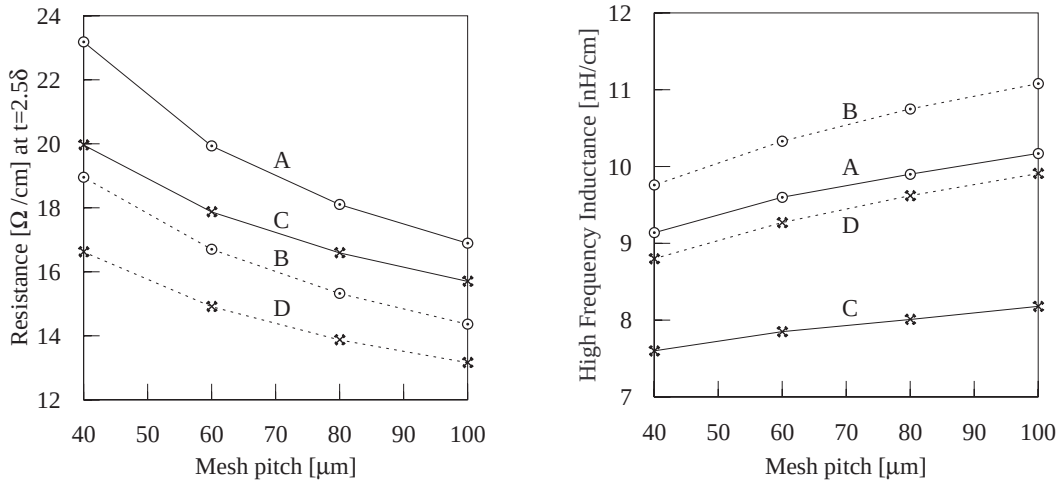

Figure 5.11: Comparison of resistance and inductance of a microstrip line over a meshed ground plane with varying mesh pitch. (a) Resistance at $t = 2.5\delta$ vs. mesh pitch, (b) High frequency inductance vs. mesh pitch. Aperture ratio = $(g / p)^2 \times 100$ [%]. A(⊙ and solid line): 3DSRM at 50% aperture, B(⊙ and dotted line): PEEC with straight line approximation at 50% aperture, C(⊠ and solid line): 3DSRM at 25% aperture, D(⊠ and dotted line): PEEC with straight line approximation at 25% aperture.

segments on each side with width ratios of 1.4 and 2, respectively, for all three segmentation schemes. These three segmentation schemes are identified as PEEC1, PEEC2, and PEEC3, respectively. 3DSRM uses uniform 7×7 segments in the xy-plane and three segments with width ratio of 2.8 for the wide surface and one segment for the narrow surface of the signal line. To reduce the number of unknowns only the top surface of the meshed ground is segmented instead of all surfaces. The strip width of the meshed ground is approximately increased by the thickness to account for the effect of finite thickness edges. This leads to 398, 283, 743 and 148 unknowns for the three PEECs and 3DSRM, respectively. For inductance 3DSRM is close to PEEC2 and PEEC3 with a deviation of 5% at low frequency and 4% at high frequency, while PEEC1 is considerably off about 23% due to the simplified geometry and overestimated line length. For resistance, 3DSRM and the PEECs are matched well up to $\delta = t$. PEEC3 is off about 20% from 3DSRM at 10 GHz because coarse segments are used on the meshed ground plane and, therefore, current crowding is underestimated. Table 5.2 compares the number of unknowns and the computation time of the various segmentation schemes and techniques used. When 3DSRM uses uniform 12×12 segments on one cell of the meshed ground plane, PEEC1 uses 6×3 segments with width ratios of 3 and 2.5, respectively, on each side of simplified straight lines, and 12×4 segments with width ratios of 1.4 and 2, respectively, on the signal line for both cases. Figure 5.11 compares resistance and inductance vs. mesh pitch. Figure 5.11(a) compares resistance at $t = 2.5\delta$ vs. mesh pitch, where PEEC1 is off about 16% from 3DSRM. Figure 5.11(b) compares high frequency inductance vs. mesh pitch, where for 25% aperture PEEC1 overestimated inductance about 20% compared to the 3DSRM and for 50% aperture PEEC1 gives a slightly higher value of 8% compared to 3DSRM. This indicates that the aperture ratio is becomes large

the simple approximation of straight lines is enough to capture the effect of the meshed ground plane, as expected. Through this example the efficiency and accuracy of 3DSRM is demonstrated by comparing the results to those of the more rigorous PEEC.

5.4 Discussion and Further Considerations

Simple EII models have been derived for three dimensional geometries by extending the transmission line model from the two dimensional problems. EII can be combined with the surface integral equations and the current continuity condition is satisfied by applying Kirchhoff's voltage law (KVL). This 3DSRM is utilized to examine three examples and the accuracy and efficiency is verified.

Even though non-equal segments are used in this study, a more optimized non-uniform discretization scheme can be developed to further enhance the efficiency of the technique. This technique has been applied to structures having rectangular cross-sections with rectangular segments, and it can be extended to the geometries of trapezoidal or circular cross-sections with developing the proper EII models. But to afford a complicated geometries like a via-hole structure [74] triangular segments can be used as in the full-wave electric field integral equation method (EFIE) of reference [10, 54]. It may require higher order of basis functions [54] than pulse basis functions and more CPU time to calculate the integral of Green's functions. The fast iterative matrix solver [64] and FFT-based [72, 73] or multipole-accelerated matrix-vector multiplication [64] can also be utilized in 3DSRM to enhance the numerical efficiency.